# Surface and interface phase transitions in thin magnetic films with frustrated exchange interactions

D. Spišák* and J. Hafner

*Institut für Theoretische Physik and Center for Computational Materials Science, Technische Universität Wien,
Wiedner Hauptstraße 8-10/136, A-1040 Wien, Austria*

(Received 4 Feburary 1997)

Detailed studies of magnetic phase transitions in thin magnetic films with frustrated exchange interactions on nonmagnetic surfaces are presented. In the first part of the work we use a self-consistent real-space tight-binding linear-muffin-tin orbital approach to determine the magnetic structure of face-centered cubic Fe films on Cu(100) substrates and a Green's-function technique to calculate the exchange pair interactions. The results demonstrate a ferromagnetic coupling at the free surface and antiferromagnetic coupling in the interior of the films. The competition between ferro- and antiferromagnetism leads to a pronounced enhancement of the exchange coupling at the surface and at the interface with the nonmagnetic substrate and a strong reduction (frustration) in the inner layers. In the second part we use these results to formulate an Ising model for magnetic films with frustrated exchange interactions and to perform extended Monte Carlo simulations of magnetic phase transitions. The results demonstrate a rich scenario of two-dimensional surface and interface phase transitions, coupled through weak magnetic fluctuations in the interior of the film. In addition, spin-reorientation transitions (reversible and irreversible) between high- and low-moment states are observed. [S0163-1829(97)05529-X]

## I. INTRODUCTION

The nature of the phase transitions at the surface of magnetic materials and in thin magnetic films has been studied repeatedly in recent years.[1–5] The main aim of these studies was to characterize the critical behavior at the surface of a magnetic material or at the interface of a magnetic film with a nonmagnetic surface and to find out whether it can be related to the properties of the bulk materials. The earliest studies in this direction were performed by Binder and Hohenberg[6] who demonstrated that in Ising and Heisenberg systems with different nearest-neighbor coupling in the bulk and at the surface distinct phase transitions can occur at the surface and in the bulk. Later extensive Monte Carlo calculations for semi-infinite three-dimensional Ising models have been used to establish the phase diagram for a material where the exchange interaction $J_s$ at the surface differs from that in the bulk.[4] It has been shown that a surface phase transition decoupled from the phase transition in the bulk can occur in two different regimes: (a) $J > 0$ and $J_s < 0$. Here the bulk is ferromagnetically ordered below a bulk critical temperature $T_{cb}$, and the interface orders antiferromagnetically at a temperature $T_{cs}$. The phase boundaries for the surface and bulk phase transitions cross at a decoupled tetracritical point. (b) $J > 0$ and $J_s > J_{sc} > J$. If the exchange coupling at the surface is much stronger than in the bulk, the surface remains ferromagnetically ordered above $T_{cb}$ and the surface phase transition shows two-dimensional critical behavior. At $J_s = J_{sc} \simeq 1.52 J$ bulk and surface become simultaneously critical and the phase boundaries meet at a different multicritical point (sometimes also referred to as the ''special transition''). Later these investigations were extended to continuous models like the classical $XY$ model[5] and it was shown that the surface transition is of the Kosterlitz-

Thouless type.[7] This also implies that the transition at the multicritical point (i.e., the ''special'' transition) has a different character.

Parallel to the progress in statistical-mechanical studies of idealized model systems, advanced experimental techniques allowed for an investigation of the magnetic properties of surfaces and ultrathin films with unprecedented accuracy.[8] In general one finds that, due to the reduced coordination number, the critical temperature is lower at the surface and in thin films and decreases with decreasing film thickness.[9–11] However, this does not represent a universal behavior as predicted by a scaling hypothesis.[12] An enhanced Curie temperature at the surface and an ordered surface coexisting with a disordered bulk has been experimentally observed for Gd.[13] For face-centred-cubic Fe films on Cu(100) substrates the Curie temperature increases strongly from one to two monolayers, but decreases in thicker layers.[14,15] In addition, different behaviors have been reported for the variation of the magnetization as a function of temperature, ranging from a linear temperature dependence[16,17] to a behavior similar to that in bulk ferromagnets with a slow variation at low temperatures and a sharp drop of the magnetization as the critical temperature is approached.[18,19] Again fcc Fe/Cu(100) films are a very interesting case for study, because the magnetization curves have been shown to change from a shape characteristic for an almost ideal anisotropic Heisenberg ferromagnet for the thinnest films [≤2 monolayers (ML)] to a linear temperature dependence in the thicker (~7 ML) films.[15]

Several attempts have been made to relate the variation of the critical temperature at the surface or in a thin film not only to the reduced coordination number, but also to surface magnetic moments $\mu_s$ and exchange coupling constants $J_{ij}^s$ deviating from their bulk values in the region of the surface or interface.[20–22] For the free surfaces of both bcc Fe and fcc

Ni the reduction of the coordination number leads to a narrowing of the $d$ band at the surface and further to an enhancement of $\mu_s$ by 20–30 % relative to the bulk value $\mu_b$.[21,23] At the interface with a Cu substrate, the Fe-interface moments show a similar enhancement,[24] whereas the Ni moments are reduced by a comparable amount.[25] Jensen et al.[20] have used a generalized mean-field theory to show that the observed thickness dependence of $T_c$ in fcc Cu/Ni/Cu(100) sandwiches may be explained in terms of the variation of the magnetic (i.e., Ni-Ni) coordination number and the magnetic moment at the Ni/Cu interface, but assuming a surface exchange coupling equal to the value in the bulk. On the other hand, in Fe/Cu(100) films a ratio of Fe surface and bulk moments as large as $\mu_s/\mu_b \sim 1.8$ has to be assumed to reproduce the maximum in the $T_c$/thickness dependence observed experimentally.[14,15] This disagreement is indicative of the special nature of the magnetic interactions in the fcc Fe films that could also lead to a peculiar nature of the magnetic phase transitions. These transitions form the central subject of this study.

Extensive experimental work on the magnetic properties of Fe films grown epitaxially on Cu(100) substrates has established a complex phase diagram, with the physical properties depending on the film thickness $t$ and other experimental parameters. It is possible to distinguish three different regions.

(a) In region I with $t \lesssim 5-6$ ML the easy axis of magnetization is perpendicular to the surface and a competition of high-moment ferromagnetic[26–34] and low moment antiferromagnetic[35,36] states has been reported. The structure of the films has been described as tetragonally distorted ($c/a < 1$ or $c/a > 1$) fcc,[37,38] and complex ($4 \times 1$) and ($5 \times 1$) reconstructions have been proposed on the basis of low-energy electron-diffraction data.[39,40]

(b) Films in region II ($6-7$ ML $\lesssim t \lesssim 10-12$ ML) remain fcc (with eventually a small tetragonal distortion[37,41,40]) and show paramagnetism or low-moment antiferromagnetism.[42] In this region the magnetic anisotropy switches from perpendicular to in-plane. The thickness where the crossover occurs depends on the preparation conditions: film prepared at low temperature (and hence probably rougher than films prepared at room temperature[34]) show in-plane anisotropy already for $t \simeq 5-6$ ML, whereas room-temperature prepared films acquire in-plane anisotropy only at 10 to 12 ML. Low-temperature prepared films with 5–6 ML show a reversible spin-reorientation transition as a function of temperature: the direction of the magnetic moment switches from perpendicular to in-plane and back as the temperature is increased and decreased.[27]

(c) Films with $t \gtrsim 10-12$ ML are bcc and ferromagnetic with in-plane anisotropy. Early local-spin-density calculations of the magnetic properties of free-standing Fe films[43–45] agree on a ferromagnetic coupling between the moments in the surface and subsurface layers and an antiferromagnetic coupling between the deeper layers. In contrast to bulk fcc and fct iron,[46] only a weak dependence of the magnetic moments on a tetragonal distortion of the film has been predicted.[45] The most recent calculations of the magnetic structure and anisotropy of Fe/Cu(100) films in regions I and II show that the scenario is in reality more complex:[24,47–49] high-moment (predominantly ferromag-

netic) and low-moment (predominantly antiferromagnetic) solutions coexist in films with more than three ML as energetically almost degenerate stable and metastable solutions, for rough films even noncollinear spin structures have been predicted.[50] The only certain feature is that the moment at the free surface is always strongly enhanced (even compared to the bulk value in bcc ferromagnetic Fe) and ferromagnetically coupled to the moments in the first subsurface layer.

These results show that in fcc Fe/Cu(100) the ferromagnetic coupling is strongly enhanced at the free surface (and eventually also at the interface with the nonmagnetic substrate), but frustrated in the interior of the film due to competing antiferromagnetic interactions. In such a case one would expect that the phase transitions at the surface or interface are effectively decoupled from the magnetic transitions in the interior of the film. In the present work this conjecture has been further explored.

Our approach consists of two distinct steps. In the first we use local-spin-density theory to calculate the magnetic structure of Fe/Cu(100) films with up to 6 ML Fe and a real-space Green's-function approach to calculate the exchange coupling between pairs of magnetic moments. This confirms both the existence of stable/metastable ferro- and antiferromagnetic configurations, and the enhancement of the exchange interactions at the surfaces, as well as their strong reduction (frustration) in the interior of the film. In the second step we map the magnetic interactions on an effective Ising-Hamiltonian and we perform extensive Monte-Carlo studies of the magnetic phase transitions. A detailed analysis of the data demonstrates the existence of surface and interface phase transitions and shows in addition that spin-reorientation transitions can lead to temperature-dependent transformations between high- and low-moment phases.

## II. MAGNETIC STRUCTURE AND EXCHANGE-PAIR INTERACTIONS IN FE FILMS ON CU(100) SUBSTRATES

### A. Theory

Our investigations of the magnetic properties of thin films are based on self-consistent spin-polarized electronic-structure calculations performed with a local-spin-density (LSD) Hamiltonian[51] in a scalar-relativistic approximation, using a real-space tight-binding linear-muffin-tin-orbital (TB-LMTO) technique.[52–54] Given the initial charge densities and potential parameters, the partial local spin-polarized densities of states (DOS's) were computed using the real-space recursion method.[55] From the moments of the DOS's integrated up to the Fermi level, the updated charge and spin densities, local magnetic moments, and potential parameters were calculated. The self-consistency iterations were stopped after the difference of all the magnetic moments in two succeeding iterations became smaller than $10^{-4} \mu_B$.

The recursion calculations were performed for large clusters of atoms with periodic boundary conditions in lateral directions and free boundary conditions in the direction of the surface normal. Each cluster consists of three layers of empty spheres to account for the spilling out of charge into the vacuum, one to six Fe layers, three Cu interface layers (in these layers charge and spin densities are calculated self-consistently) plus up to six Cu layers with the potential parameters fixed at the values characteristic for bulk Cu. The

interatomic distance is equal to that in bulk Cu, no relaxation in the Fe overlayer has been allowed. Each fcc (001) layer contains 288 atoms in a $(12\sqrt{2}\times12\sqrt{2})$ cell. Twenty exact recursion levels in the continued fraction were used for $s$ and $p$ states, 40 recursion levels were used for $d$ states. The Beer-Pettifor terminator[56] was used to get a smooth DOS.

Recently we have shown[21,22] that the real-space tight-binding approach may be used for an efficient calculation of the exchange-pair interactions $J_{ij}$ between the local magnetic moments $\mu_i$, following the torque-force approach pioneered by Small and Heine.[57] The exchange coupling between a pair of magnetic moments at sites $i$ and $j$ can be expressed as

$$J_{ij}=\frac{\Delta_i\Delta_j}{2\pi}\mathrm{Im}\int_{-\infty}^{E_F}\mathrm{Tr}G_{ij}^{\uparrow\uparrow}G_{ji}^{\downarrow\downarrow}dE, \tag{1}$$

where $\Delta_i$ stands for the local exchange splitting and where $G_{ij}^{ss'}$ is an intersite Green's function of the system in the ground state. In principle this is equivalent to a mapping of the LSD Hamiltonian of an itinerant $3d$ magnet on a classical Heisenberg spin Hamiltonian describing a localized magnet. Independently, a closely related approach to the exchange-pair interactions has recently been proposed by Mryasov et al.[58]

We have recently used this approach (and its generalization to biquadratic exchange coupling) to calculate the exchange interactions in bulk bcc ferromagnetic Fe, at Fe surfaces[21] and at the interface of ferromagnetic Fe substrates with antiferromagnetic Mn overlayers.[22] For the present context, the main results of these studies (besides the confirmation that good agreement with experimentally measured spin-wave stiffness constants and related properties can be achieved) are (i) The exchange-pair interactions are long ranged. Quantitatively converged values for Curie temperatures, spin-wave parameters, etc., can be achieved only after taking the sum over 12–15 shells of neighbors. (ii) Like the magnetic moments, both the nearest- and next-nearest-neighbor exchange interactions are strongly enhanced at the surface [the nearest-neighbor interaction in the (001) surface increases from $J=16.27$ meV in the bulk to $J_s=44.30$ meV in the surface and $J_{s-1}=18.14$ meV in the subsurface layer, the moment from $\mu_b=2.21\mu_B$ to $\mu_s=3.04\mu_B$ and $\mu_{s-1}=2.09\mu_B$)]. (iii) The reduced coordination numbers and the enhanced moments and exchange couplings have opposite effects on the local Curie temperature. Within a mean-field approximation, the highest transition temperature is calculated not for the surface but for the first subsurface layer. (iv) These results, together with the fact that the nearest-neighbor coupling is enhanced not only *in*, but also perpendicular to the surface layer indicates that in a realistic surface the decoupling of surface and bulk-phase transitions might be more difficult to achieve than in a model where only the in-plane coupling is enhanced.

## B. Coexisting high- and low-spin solutions

Table I summarizes our results for the layer-resolved magnetic moments in the Fe/Cu(100) films, together with the earlier $\vec{k}$-space LMTO and $\vec{r}$-space TB-LMTO results of Lo-

renz and Hafner[24,47] and the results of Ujfallussy et al.[48] and Szunyogh et al.[49] based on a relativistic screened Kohn-Korringa-Rostoker (KKR) technique. Coexisting low- and high-spin solutions were first found for 5 and 7 ML films using a technique allowing for a continuous rotation of the local spin quantization axes which makes it easier to relax the spin-configuration to the ground state. These calculations have been performed using a Hubbard-Stoner-type exchange Hamiltonian[59] — this explains the slightly different values for the moments obtained here with the full LSD Hamiltonian. The KKR calculations are based on a fully relativistic Hamiltonian and have been performed for ferro- as well as antiferromagnetic configurations at all thicknesses.

The appearance of both ferromagnetic high-spin and partially antiferromagnetic (AFM) low-spin solutions in fcc Fe films is, of course, closely related to the frustrated exchange interactions in bulk fcc Fe. Depending on the atomic volume, a constrained collinear calculation results in stable/unstable low/high-spin AFM configurations. However, at least for a wide range of densities, the magnetic ground state is definitely a noncollinear state, probably a spin spiral.[58,60,61] In ideally flat Fe films, the calculations of Lorenz and Hafner[24,47] have so far not found any indications for a possible noncollinear solution.

For films with one and two monolayers all calculations agree on a ferromagnetic ground state with strongly enhanced moments. For a three-layer film we find three metastable solutions: the low-spin solution with an antiferromagnetic coupling close to the substrate (we adopt the notation $\uparrow\uparrow\downarrow$, starting from the free surface and proceeding towards the substrate) is marginally lower in energy than the ferromagnetic high-spin solution $\uparrow\uparrow\uparrow$. The symmetrical low-spin solution $\uparrow\downarrow\uparrow$ leads to a strongly reduced moment in the central layer. This is a consequence of the frustration of the interactions between the surface and subsurface layer. Such a solution is stabilized in an Fe-film sandwiched between thick Cu layers.[49]

For a four-layer film both TB-LMTO calculations (with Hubbard-Stoner and LSD exchange, respectively) converge to the configuration $\uparrow\uparrow\downarrow\uparrow$ with ferromagnetic coupling at the surface and antiferromagnetic coupling in the deeper layers. However, both calculations and the KKR result disagree on the degree of quenching of the antiferromagnetic moments. We have verified that both sets of calculations are well converged with respect to the local minimum, hence these results indicate a very flat distribution of the total energy independence on the magnetic moments.

For the 5 ML film the ground state is the low-spin configuration $\uparrow\uparrow\downarrow\uparrow\downarrow$ that was also found in the KKR calculations, but according to Lorenz and Hafner[24,47] a high-spin solution $\uparrow\uparrow\uparrow\downarrow\uparrow$ with only a single antiferromagnetic layer is almost equal in energy. For the 6 ML film all calculations agree on a ground-state configuration $\uparrow\uparrow\downarrow\downarrow\uparrow\uparrow$ with antiferromagnetically coupled double layers, enhanced moments in the outer layers and quenched moments in the interior of the film. However, here again slight differences in the setup (scalar-relativistic $\leftrightarrow$ fully relativistic, LSD-exchange $\leftrightarrow$ Hubbard-Stoner exchange) result in relatively large differences in the magnitude of the quenched moments.

TABLE I. Average magnetic moment $\langle m \rangle$ and layer-resolved magnetic moments $m_i$ (in $\mu_B$)

### (a) LMTO calculation (after Ref. 24)

| l | 1 | 2 | 3 | 4 | $5_1$ | $5_2$ | 6 |
|---|---|---|---|---|---|---|---|
| $\langle m \rangle$ | 2.72 | 2.70 | 2.65 | 1.40 | 1.59 | 0.56 | 0.87 |
| $m_1$ | 2.72 | 2.86 | 2.87 | 2.86 | 2.92 | 2.79 | 2.81 |
| $m_2$ | | 2.53 | 2.50 | 2.40 | 2.49 | 2.24 | 2.28 |
| $m_3$ | | | 2.58 | −2.01 | 2.42 | −1.68 | −2.38 |
| $m_4$ | | | | 2.35 | −2.24 | 1.69 | −2.35 |
| $m_5$ | | | | | 2.35 | −2.26 | 2.32 |
| $m_6$ | | | | | | | 2.54 |

### (b) TB-LMTO calculation (after Ref. 24)

| l | 1 | 2 | 3 | 4 | 5 | 6 |
|---|---|---|---|---|---|---|
| $\langle m \rangle$ | 2.71 | 2.49 | 2.45 | 1.41 | 0.58 | 0.82 |
| $m_1$ | 2.71 | 2.76 | 2.82 | 2.81 | 2.75 | 2.77 |
| $m_2$ | | 2.22 | 2.34 | 2.38 | 2.27 | 2.20 |
| $m_3$ | | | 2.19 | −1.95 | −1.70 | −2.36 |
| $m_4$ | | | | 2.41 | 1.86 | −2.31 |
| $m_5$ | | | | | −2.27 | 2.11 |
| $m_6$ | | | | | | 2.51 |

### (c) KKR calculation – ferromagnetic solution (after Ref. 48)

| l | 1 | 2 | 3 | 4 | 5 | 6 |
|---|---|---|---|---|---|---|
| $\langle m \rangle$ | 2.78 | 2.69 | 2.62 | 2.56 | 2.54 | 2.53 |
| $m_1$ | 2.78 | 2.79 | 2.82 | 2.83 | 2.84 | 2.85 |
| $m_2$ | | 2.59 | 2.49 | 2.47 | 2.49 | 2.50 |
| $m_3$ | | | 2.56 | 2.38 | 2.39 | 2.42 |
| $m_4$ | | | | 2.54 | 2.43 | 2.41 |
| $m_5$ | | | | | 2.55 | 2.45 |
| $m_6$ | | | | | | 2.56 |

### (d) KKR calculation – antiferromagnetic solution (after Ref. 49)

| l | 1 | 2 | 3 | 4 | 5 | 6 |
|---|---|---|---|---|---|---|
| $\langle m \rangle$ | 2.78 | 0.01 | 1.00 | 1.47 | -0.55 | 0.92 |
| $m_1$ | 2.78 | 2.36 | 2.82 | 2.79 | -2.79 | 2.79 |
| $m_2$ | | −2.34 | 2.30 | 2.26 | -2.25 | 2.16 |
| $m_3$ | | | −2.12 | −1.43 | 1.51 | −2.02 |
| $m_4$ | | | | 2.26 | −1.45 | −2.03 |
| $m_5$ | | | | | 2.22 | 2.09 |
| $m_6$ | | | | | | 2.52 |

### (e) TB-LMTO calculation (present results), the index 1 indicates the ground state

| l | 1 | 2 | $3_1$ | $3_2$ | $3_3$ | 4 | 5 | 6 |
|---|---|---|---|---|---|---|---|---|
| $\langle m \rangle$ | 2.76 | 2.60 | 0.93 | 1.13 | 2.44 | 1.37 | 0.49 | 0.92 |
| $m_1$ | 2.76 | 2.77 | 2.80 | 2.50 | 2.81 | 2.81 | 2.79 | 2.74 |
| $m_2$ | | 2.43 | 2.03 | -1.22 | 2.09 | 1.92 | 1.85 | 1.78 |
| $m_3$ | | | −2.05 | 2.10 | 2.42 | −1.36 | −1.40 | −1.64 |
| $m_4$ | | | | | | 2.10 | 1.30 | −1.68 |
| $m_5$ | | | | | | | −2.08 | 1.85 |
| $m_6$ | | | | | | | | 2.33 |

### (f) MC simulation (present results), the index 1 indicates the ground state

| l | 1 | 2 | 3 | 4 | $5_1$ | $5_2$ | $6_1$ | $6_2$ |
|---|---|---|---|---|---|---|---|---|
| $m_1$ | ↑ | ↑ | ↑ | ↑ | ↑ | ↑ | ↑ | ↑ |
| $m_2$ | | ↑ | ↑ | ↑ | ↑ | ↑ | ↑ | ↑ |
| $m_3$ | | | ↑ | ↑ | ↓ | ↑ | ↓ | ↓ |
| $m_4$ | | | | ↑ | ↓ | ↑ | ↓ | ↑ |
| $m_5$ | | | | | ↓ | ↑ | ↑ | ↓ |
| $m_6$ | | | | | | | ↑ | ↓ |

## C. Effective exchange coupling

Table II summarizes our results for the nearest- and next-nearest exchange interactions in the Fe/Cu(100) films. The exchange coupling has been calculated for the ground state. As in bulk Fe and at Fe surfaces, the exchange interactions are quite long ranged, but for clarity we report only the dominant short-range interactions where the enhancement due to the reduced coordination close to the surface or interface is most pronounced.

In the monolayer limit we note a huge enhancement of the nearest-neighbor (NN) exchange coupling: $J^{NN}=42.2$ meV, compared to $J^{NN}=16.3$ meV in bulk ferromagnetic (FM) Fe, comparable to $J^{NN}=44.3$ meV at the surface of FM bcc Fe (see Ref. 21). Even the next nearest-neighbor (NNN) interaction in the monolayer is stronger than the nearest-neighbor coupling in the bulk. The surface-related enhancement of the NN coupling within the layers is only slightly weaker in a 2 ML slab, but the interlayer coupling is almost the same as in the bulk. At the interface with the Cu substrate we note a relatively weak NNN coupling.

The effect of competing ferro- and antiferromagnetic polarizations appears first in the 3 ML film. The intralayer interactions in the surface and interface layers are both enhanced over the bulk values, more strongly at the free surface than at the interface. The asymmetry can be attributed mainly to the different behavior of the $s,p$ electrons at the surface and at the interface. For the bulk our analysis[21] has shown that the strong FM $d$-$d$ coupling is partly reduced by negative $s,p$-$d$ contributions. At the surface, the $s,p$ electrons partly relax into the vacuum and the enhancement of the $d$-$d$ coupling due to a narrower $d$ band is fully effective. No $s,p$ relaxation occurs at the interface and the Fe-$d$–Cu-$d$ hybridization limits the narrowing of the Fe-$d$ band. Within the central Fe layer the exchange coupling is comparable to that in the bcc Fe bulk (the different atomic structure of the film seems to be of minor importance). The most interesting effect, however, is the competition between the strong AFM-NNN coupling between the surface and interface layer ($J^{NNN}_{S-(S-2)}=-22.0$ meV) and the FM-NN coupling between the central and the interface layer ($J^{NN}_{(S-1)-(S-2)}=10.8$ meV). While the former interaction favors the low-spin ↑↑↓ configuration, the latter favors the high-spin FM ↑↑↑ configuration. In either configuration, one of these interactions is necessarily frustrated.

In the 4 ML film the intralayer couplings in the surface and interface layers are about the same as in the 3 ML film, the coupling in the subsurface layer is bulklike. The most striking effect is the extremely weak exchange coupling within the antiferromagnetically polarized third layer. The antiferromagnetic moments are stabilized by a strong AFM-NNN coupling to the surface-layer ($J^{NNN}_{S-(S-2)}=-12.5$ meV), and a weaker AFM-NN coupling to the interface layer. In the ↑↑↓↑ configuration the FM-NN coupling between the second and third layers is necessarily frustrated.

A similar situation is established for the 5 ML film in the ↑↑↓↑↓ ground state: enhanced coupling within surface and interface layers, bulklike interactions in the subsurface layer, very weak exchange interactions in the third and fourth layers in the interior of the film. This concerns not only the intralayer coupling, but the interlayer coupling as well. The

TABLE II. Effective exchange parameters $J^{NN}(l)$, $J^{NN}(l+1)$ and $J^{NNN}(l)$, $J^{NNN}(l+1)$ (in meV). NN stands for nearest-neighbor, NNN for next-nearest-neighbor coupling, $l$ for coupling within the same layer, $l+1$ for coupling to an atom in the neighboring layer.

| No. of Layers | Layer | Orientation | $J^{NN}(l)$ | $J^{NNN}(l)$ | $J^{NN}(l+1)$ | $J^{NNN}(l+2)$ |
|---|---|---|---|---|---|---|
| 1 | 1 | ↑ | 42.20 | 19.19 | | |
| 2 | 1 | ↑ | 37.67 | 14.11 | 18.26 | |
|   | 2 | ↑ | 37.65 | 9.15 | | |
| 3 | 1 | ↑ | 29.02 | 9.86 | 19.37 | −22.04 |
|   | 2 | ↑ | 15.80 | 7.77 | 10.79 | |
|   | 3 | ↓ | 20.66 | 9.62 | | |
| 4 | 1 | ↑ | 31.26 | 8.59 | 13.61 | −12.54 |
|   | 2 | ↑ | 11.76 | 5.94 | 2.62 | 7.25 |
|   | 3 | ↓ | −0.22 | 3.59 | −4.51 | |
|   | 4 | ↑ | 19.71 | 10.08 | | |
| 5 | 1 | ↑ | 29.16 | 7.58 | 12.56 | −12.88 |
|   | 2 | ↑ | 11.64 | 5.48 | 3.92 | 2.05 |
|   | 3 | ↓ | −2.12 | 3.91 | −4.26 | 6.11 |
|   | 4 | ↑ | −1.75 | 3.00 | −3.32 | |
|   | 5 | ↓ | 19.36 | 10.86 | | |
| 6 | 1 | ↑ | 23.63 | 6.99 | 12.45 | −14.64 |
|   | 2 | ↑ | 12.91 | 7.16 | 9.40 | −5.28 |
|   | 3 | ↓ | −0.28 | 7.75 | 5.66 | −7.47 |
|   | 4 | ↓ | 1.28 | 7.50 | 9.22 | −10.29 |
|   | 5 | ↑ | 10.04 | 8.97 | 5.64 | |
|   | 6 | ↑ | 23.41 | 11.44 | | |

↑↑↓↑↓ spin configuration is stabilized mainly by a strong AFM-NNN coupling between the surface and the third layer ($J^{NNN}_{S-(S-2)} = -12.9$ meV), a modest FM-NNN coupling of this layer to the interface layer ($J^{NNN}_{(S-2)-(S-4)} = 6.1$ meV), as well as weaker AFM-NN interlayer couplings in the deeper layers. The FM-NN coupling between layers (S-1) and (S-2) is frustrated in this configuration.

A different scenario appears for the AFM coupled double layers forming the ↑↑↓↓↑↑ ground state of the 6 ML film. In this almost symmetric configuration we find enhanced intra-layer interactions in surface and interface layers, bulklike interactions in the adjacent layers, and quenched interactions in the paired central layers (but note the relatively strong FM-NNN intralayer coupling). All NN-interlayer interactions are ferromagnetic, all NNN-interlayer interactions are antiferromagnetic and stronger than the FM-NN interactions if a surface or interface layer is involved. This leads naturally to the ↑↑↓↓↑↑ double-layer configuration where only every fourth NN or NNN interlayer interaction is frustrated.

Altogether our results demonstrate that due to the existence of frustrated ferro- and antiferromagnetic exchange interactions in fcc Fe, the magnetic interactions in fcc Fe$_n$/Cu(100) films are much more complex than assumed in the simple scenario underlying previous studies of magnetic surface phase transitions. Strongly enhanced interactions near the surface or interface, quenched coupling in the interior of the films suggest the occurrence of surface and eventually also interface phase transitions. Antiferromagnetic NNN interlayer interactions that are even stronger than the

ferromagnetic NN interlayer coupling indicate the possibility of even more complex transitions. In the following these magnetic transitions will be studied using Monte Carlo simulations.

However, this is not an easy task: the exchange-pair interactions we have calculated are, in principle, Heisenberg-type and long ranged. Monte Carlo simulations for all 1–6 ML films, on ensembles that are sufficiently large to allow for a characterization of the magnetic phase transitions, would hence be prohibitively expensive. We therefore decided to simplify the task by (a) restricting the interactions to nearest- and next-nearest-neighbor sites (as given in Table II), and (b) performing the simulations for an Ising instead of a Heisenberg model. This leads to a tractable model. The cutoff operated on the range of these interactions could, in principle, be compensated in part by a renormalization of the short-range interactions such that the critical temperatures are correctly described. Here we do not proceed to a renormalization, but the necessity should be kept in mind before making any comparisons with experiment. To use an Ising instead of a Heisenberg model appears to be a more serious limitation, especially as the exchange interactions have been calculated for an infinitesimal rotation of the moments. However, previous Ising as well as Heisenberg MC simulations with a fixed set of exchange interactions for an AFM Mn ML on a Fe(100) substrate[22,62] show that both simulations lead to equivalent scenarios for the magnetic transition, although the critical temperature scales by about a factor of 2. Hence Ising-MC simulations should be sufficient to characterize the
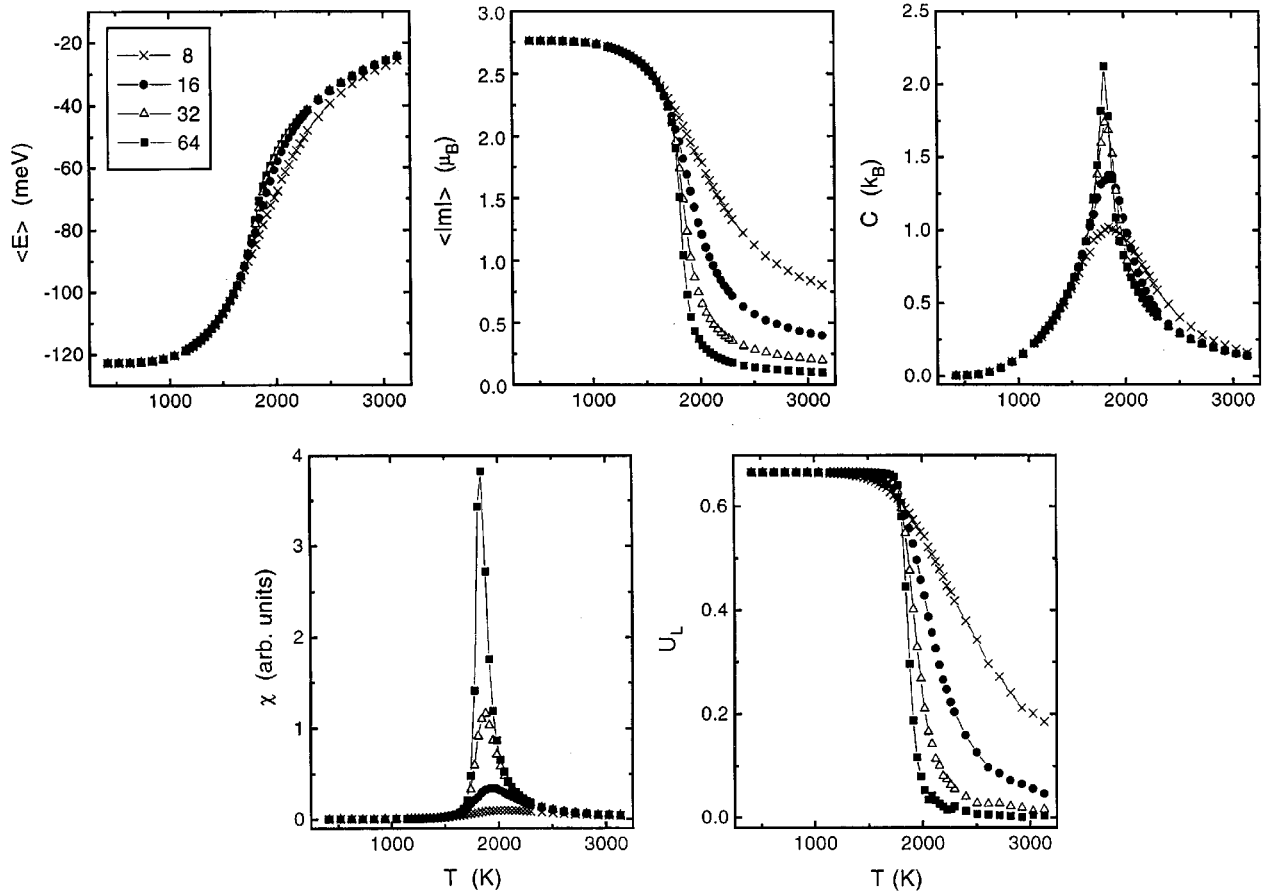
FIG. 1. Variation of the internal energy $\langle E \rangle$, the average magnetization per atom $\langle |m| \rangle$, the specific heat $C$, the susceptibility $\chi$, and the fourth-order cumulant $U_L$ with temperature, calculated for a monolayer of Fe on top of a nonmagnetic Cu substrate. The size of the model has been varied from $8 \times 8$ to $64 \times 64$.

possible phase transitions in a qualitative manner, but the results should be taken as a representative model of magnetic films with frustrated exchange interactions, and not immediately for Fe films on Cu substrates.
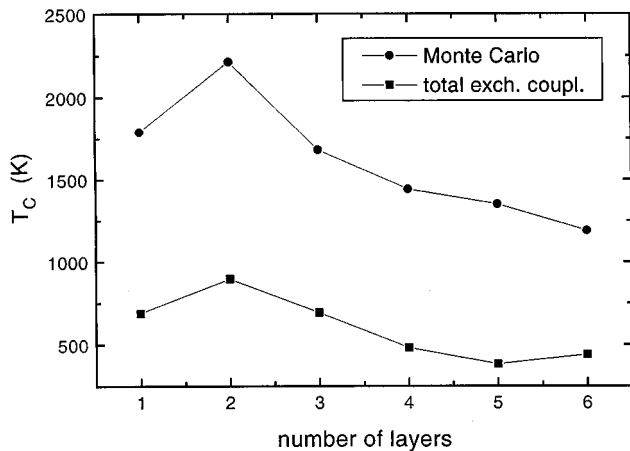


FIG. 2. Variation of the critical temperature $T_c$ with the nmber of monolayers in the Fe film, calculated using Monte Carlo simulations and truncated nearest- and next-nearest-neighbor interactions (as given in Table II), and calculated using mean-field theory and long-range exchange coupling. Cf. text.

## III. ISING MONTE CARLO STUDIES OF PHASE TRANSITIONS IN THIN FILMS

### A. Background

Our simulations are based on a three-dimensional Ising Hamiltonian with the moments listed in Table I and the NN and NNN exchange couplings listed in Table II. The simulations were carried out for ($L \times L$) cells in the film plane ($L = 8,16,32,64$) and 1–6 layers thick. Periodic boundary conditions were applied parallel to the surfaces, free boundary conditions to both top and bottom surfaces. A standard single spin-flip Monte Carlo method with a Metropolis algorithm for the flipping probability[63] was used. Data sampling was extended over $8 \times 10^4$ ($L = 8$) up to $12 \times 10^5$ ($L = 64$) MC steps.

For each film we report the variation of the average energy $\langle E \rangle$, the average magnetic moment $\langle |m| \rangle$, the specific heat $C$, and of the susceptibility $\chi$ with temperature. The specific heat and susceptibility were calculated according to the fluctuation-dissipation theorem as

$$C = \frac{\langle E^2 \rangle - \langle E \rangle^2}{k_B T^2} \tag{2}$$

and
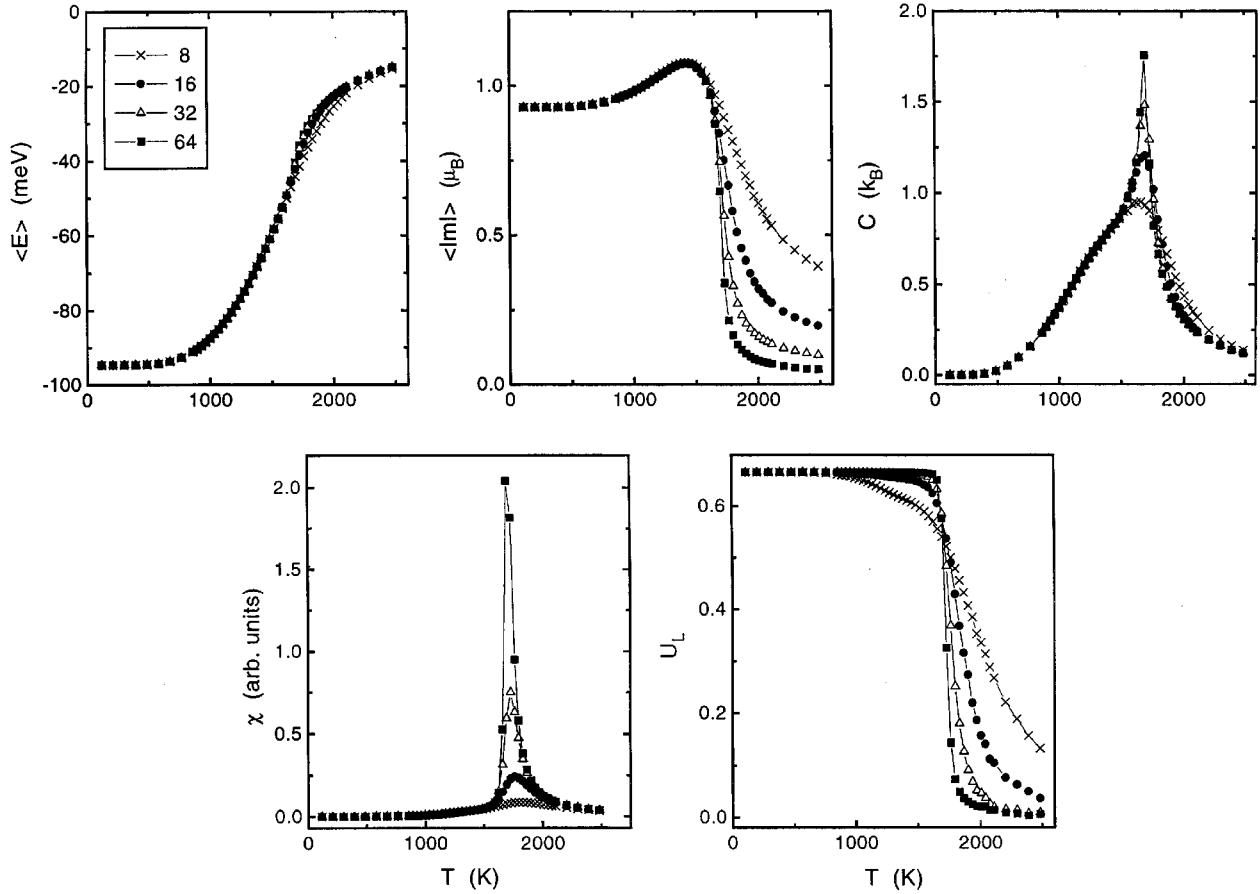
FIG. 3. Summary of the MC simulations for the 3 ML-Fe/Cu(100) film, cf. Fig. 1.

$$\chi = \frac{\langle m^2 \rangle - \langle |m| \rangle^2}{k_B T} . \tag{3}$$

Another important quantity for determining the transition temperature is the fourth-order cumulant $U_L$ defined as[64]

$$U_L = 1 - \frac{\langle m^4 \rangle_L}{3 \langle m^2 \rangle_L^2} . \tag{4}$$

A convenient method for locating the phase transition is to follow the variation of $U_L$ with temperature for various $L$ and to look where these curves intersect.

In addition to the quantities characterizing the global properties of the films, we monitor also the layer-resolved average moments $\langle |m_i| \rangle$ and susceptibilities $\chi_i$ again as determined from the fluctuation of the moments in the respective layer. The layer moments and susceptibilities display critical behavior with characteristic exponents and amplitudes,

$$m_i = B_i t_i^\beta \tag{5}$$

$$\chi_i = C_i t_i^\gamma , \tag{6}$$

where $t = |1 - T/T_{ci}|$. The local critical temperature $T_{ci}$ agrees with the critical temperature $T_{cf}$ of the entire film only if the coupling between the layers is comparable to the intralayer coupling. Whether two-dimensional phase transi-

tions, decoupled from the global magnetic properties of the film, can occur is one of the central objectives of this study.

## B. Results

### 1. Mono- and bilayer films

The Fe monolayer is expected to behave as a classical two-dimensional (2D) Ising ferromagnet, and this is confirmed by our results compiled in Fig. 1. From the cumulant analysis we determine a critical temperature $T_c(1\,\mathrm{ML}) = 1784$ K, the analysis of the magnetization in the vicinity of the critical point leads to a critical exponent in good agreement with the 2D Ising exponent $\beta = 1/8$. Essentially identical results are obtained for a 2 ML film. The critical temperature is even higher, $T_c(2\,\mathrm{ML}) = 2214$ K. Again this is as expected, because the intralayer coupling is almost the same in both layers, and the interlayer coupling is reduced only by a factor of 2 (compare Table II). The high values of the critical temperatures are due to the cutoff of the exchange interactions. If we calculate $T_c$ from the total long-range exchange interactions according to mean-field theory,

$$T_c = \frac{1}{3k_B} \sum_i J_i = \frac{1}{3k_B} \sum_{\substack{i,j \\ j \neq i}} J_{ij} , \tag{7}$$

we obtain critical temperatures that are lower by more than a factor of 2. Figure 2 shows that this scaling factor holds not only for the mono- and bilayer case, but for all film thick-
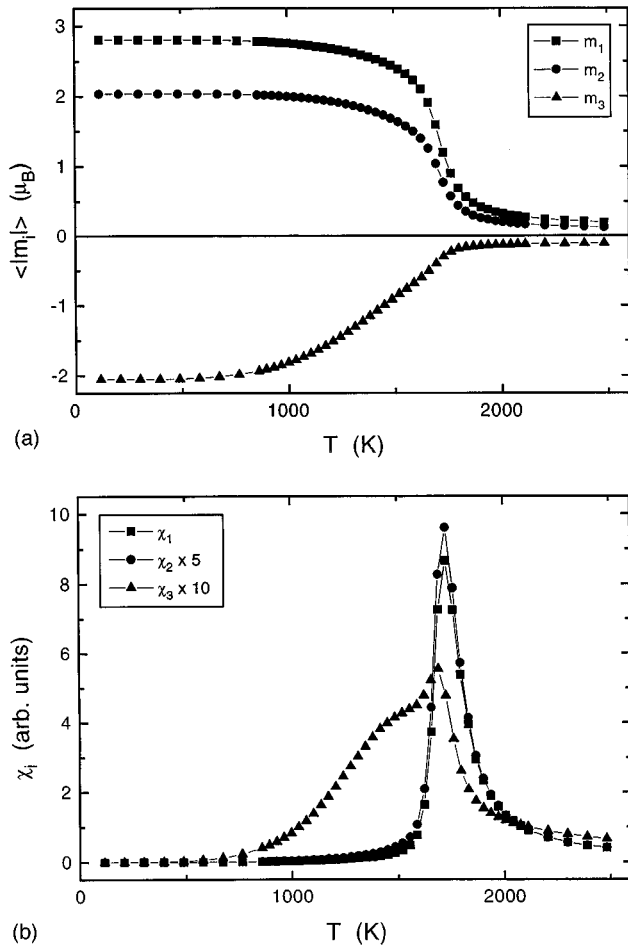
FIG. 4. Layer-resolved average moments $\langle |m_i| \rangle$ (a) and susceptibilities $\chi_i$ (b) in a 3 ML-Fe/Cu(100) film ($32 \times 32 \times 3$ lattice). The layer moments $\langle |m_i| \rangle$ have been multiplied with the sign corresponding to the global magnetization in each layer.

nesses covered in our study. Hence, in principle, the interactions could be renormalized by this factor if one wants to proceed to a more direct comparison with experimental results. Note that the trend reflects the initial increase of $T_c$ up to two layers, and the decrease for thicker layers observed in Fe/Cu(100). However, for the correct interpretation of $T_c$, see below.

### 2. 3 ML films

In the three-monolayer films with the $\uparrow\uparrow\downarrow$ ground-state configuration, we observe a more complex behavior: at the critical temperature of $T_c(3\,\mathrm{ML}) = 1680$ K, the magnetization increases first rapidly but goes through a maximum about 250 K below the critical point and saturates at a lower level. Specific heat and susceptibility show that characteristic critical divergences (see Fig. 3) occur at $T_c$, the specific heat shows in addition a broad shoulder at the low-T side of the critical peak. The analysis of the layer-resolved moments and susceptibilities (Fig. 4) demonstrates that the critical point corresponds to the paramagnetic (PM) to ferromagnetic transition in the ferromagnetically coupled surface and subsurface layers. The magnetic moments of the interface layer show no critical behavior, but only a linear increase below the critical temperature of the two overlayers. This linear

increase and the antiferromagnetic orientation is induced by the strong AFM coupling between surface and interface layers, the approach to saturation is slowed down because of the frustrated FM coupling between interface and subsurface layer (see Table II). Hence a true phase transition occurs only in the two top layers, whereas the frustration suppresses a phase transition in the interface layer.

### 3. 4 ML films

The scenario for the magnetic ordering in the 4 ML films is even more complex: from the cumulant analysis (see Fig. 5) we determine a critical temperature of $T_c(\mathrm{surface})(4\ \mathrm{ML})$ $= 1441$ K, and specific heat and susceptibility show critical behavior at this temperature. The average magnetization, however, approaches saturation only very slowly, and the specific heat shows two side maxima at lower temperatures. From the analysis of the layer-resolved moments and susceptibilities (Fig. 6) we learn that again the critical point corresponds to the PM-FM transition in the strongly coupled surface and subsurface layers. The interface layer orders ferromagnetically at a lower temperature of $T_c(\mathrm{interface}) \sim 1200$ K estimated from the peak in the layer susceptibility $\chi_4$. (At this point it is necessary to point out that the total susceptibility $\chi$ is not simply the sum of the layer susceptibilities. Interlayer correlations (here mainly between surface and subsurface layer) can make quite important contributions.) The ratio of the two transition temperatures corresponds roughly to the strengths in the exchange coupling in the surface bilayer and in the interface layer. The PM-FM transition in the interface layer is somewhat sluggish. The approach to the saturation of the magnetic moments in the interface layer does not represent a genuine two-dimensional PM-FM phase transition. This is indicated by the absence of a corresponding peak in the specific heat and the smearing of the peak in the suceptibility. The reason is that the coupling to the surface bilayer (across the magnetically essentially ''dead'' interior of the film) ordered already at higher temperatures creates a magnetic field acting on the interface moments. It is well known that an Ising ferromagnet in a magnetic field does not show critical behavior, because there is a nonzero magnetization above $T_c(\mathrm{interface})$. A magnetic moment in the (S-2) layer develops only slowly because of competing couplings to the neighboring layers. Note also that the MC simulation converges to a ferromagnetic configuration and not to the $\uparrow\uparrow\downarrow\uparrow$ configuration determined as the ground state in the LSD calculations. Altogether our results raise interesting questions concerning the character of the phase transitions in two weakly coupled two-dimensional ferromagnets which certainly deserve further investigations.

### 4. 5 ML films

Fluctuation effects are found to have a large effect on the ordering transitions in the 5 ML films. Simulations for a ($8 \times 8 \times 5$) ensemble show an onset of a magnetic ordering transition at $T_c \sim 1350$ K, but then strong fluctuations of the total magnetization in the temperature range between 750 and 500 K before the moments converge to a high-spin solution where all layers are ferromagnetically aligned [Fig. 7(a)]. Simulations performed on a ($16 \times 16 \times 5$) ensemble
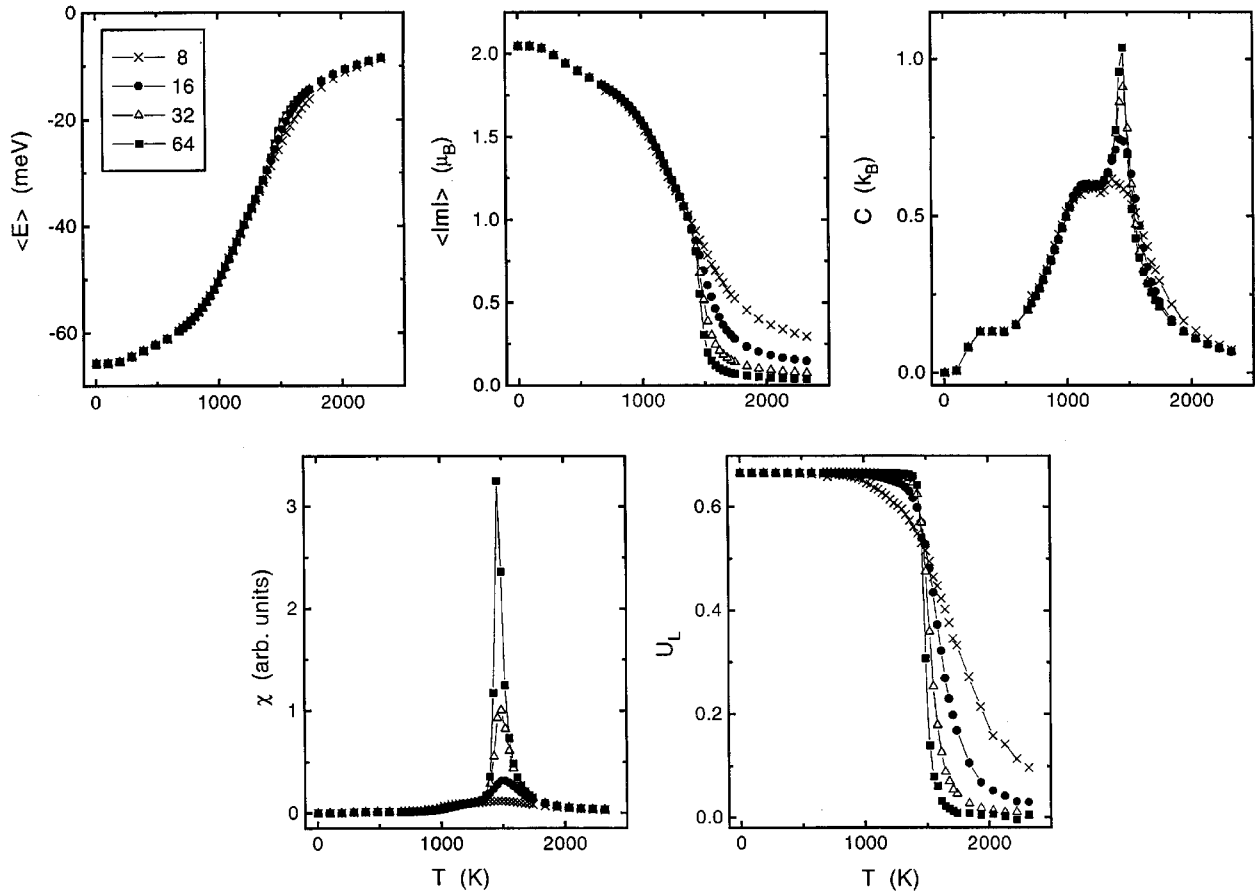
FIG. 5. Summary of the MC simulations for the 4 ML-Fe/Cu(100) film, cf. Fig. 1 and text.

follow first the same pattern, but at the temperature where the fluctuations in the smaller ensemble begin, the average magnetization breaks down and the simulation converges to a $\uparrow\uparrow\downarrow\downarrow$ configuration with almost zero total moment. Hence the breakdown of the total magnetization is the signature of a spin-reorientation transition in part of the film. Simulations for a still larger ($32\times32\times5$) ensemble converge to the ferromagnetic high-spin solution, but the variations of the shape of the magnetization vs temperature curve, the specific heat, and the susceptibility indicate that there are at least two, if not three distinct transitions. The ferromagnetic $\uparrow\uparrow\uparrow\uparrow\uparrow$ and the layered antiferromagnetic $\uparrow\uparrow\downarrow\downarrow$ configurations differ in energy by only about 1 meV/atom (with the low-spin solution being slightly lower in energy), but none of the two agrees with one of the stable or metastable $\uparrow\uparrow\downarrow\uparrow\downarrow$ and $\uparrow\uparrow\uparrow\downarrow\uparrow$ configurations found in the LSD calculations (cf. Table I).

The system can also be driven reversibly through the reorientation transition [see Fig. 7(b)], an analysis of the specific heat, susceptibility, and the cumulants indicates a sequence of three transitions ($\hat{=}$ three peaks in the specified heat). At the two high-temperature transitions, the singularity in the specific heat shows the dependence on the size of the MC ensemble expected for a second-order phase transition, whereas the low-temperature transition is almost size independent and hence does not correspond to a genuine phase transition. Figure 8(a) shows the temperature dependence of the layer-resolved magnetic moments for the transition to the

high-spin state. We find that, as in the 4 ML film, two distinct PM-FM transitions occur: first at $T_c$(surface)$\sim$1350 K in the surface bilayer, than at $T_c$(interface)$\sim$900 K in the interface layer. The second transition is now much sharper than in the 4 ML film because the two "magnetically dead" layers in the interior of the film decouple the surface and interface more effectively. The moments in the third and fourth layers do not show critical behavior, they are induced by the weak coupling to the magnetic layers.

For the PM-FM surface phase transition the susceptibility shows a size-dependent singularity coincident with the singularity in the specific heat [see Figs. 7(a,b)]. For the PM-FM interface phase transition the singularities in the susceptibility and in the specific heat coincide only for those runs for the ($32\times32\times5$) ensemble bypassing the spin-reorientation transition [see Fig. 7(a)]. If a spin reorientation takes place, it is signaled by a dominant peak in the total susceptibility at temperatures that are lower than the critical temperatures $T_c$(interface)$\sim$900 K for the interface phase transition [$T\sim$750 K for the ($16\times16\times5$) ensemble]. In this case the broad susceptibility peak of the reorientation transition covers the singularity associated with the PM-FM interface transition. This singularity is, however, clearly resolved in the layer-decomposed susceptibilities [see Fig. 8(c)] where the reorientation transition is not manifest because it involves mainly a change in the interlayer coupling. Note that the reorientation transition is not signaled by a singularity in the specific heat.
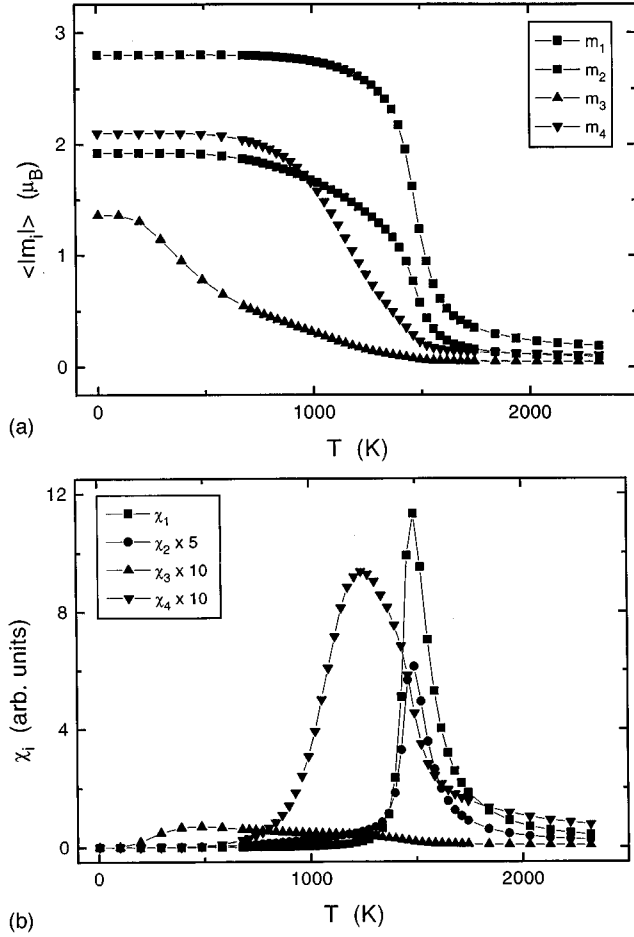
FIG. 6. Layer-resolved average moments $\langle|m_i|\rangle$ (a) and susceptibilities $\chi_i$ (b) for a 4 ML-Fe/Cu(100) film ($32\times32\times4$ lattice). Cf. text.

The transition to the low-spin state occurs through a sudden flipping of the moments in the fifth to third layers after reaching a value close to saturation [see Fig. 8(b)]. Such a spin flip would be favored by the AFM-NNN coupling of the surface to the central layer and the FM-NNN coupling of the central layer, while frustrating the weaker NN interlayer coupling (cf. Table II). These results suggest that the reorientation transition is not a phase transition in the thermodynamic sense, but merely a transition between two different metastable relative orientations of two ferromagnetic layers coupled via weak magnetic fluctuation in the interlayer.

The layer-resolved susceptibilities [Fig. 8(c)] show that the surface and interface phase transitions are neatly decoupled. The critical exponents of the magnetization close to the critical points are analyzed in Fig. 8(d). While for the interface phase transition the critical exponent ($\beta\sim0.150$) is close to the value expected for a 2D-Ising critical point, the effective critical exponents determined for the surface and subsurface layers are distinctly larger. This indicates that in the surface bilayer the coupling is no longer strictly two-dimensional.

### 5. 6 ML films

On cooling, the magnetization of the 6 ML-Fe/Cu(100) goes through a maximum slightly below the critical tempera-

ture $T_c$(6 ML)$\sim$ 1315 K estimated from the cumulant analysis and converges to a low-spin $\uparrow\uparrow\downarrow\uparrow\downarrow\downarrow$ configuration with an average moment of only $0.06\mu_B$/atom (Fig. 9). This configuration is about 4 meV/atom higher in energy than the symmetric $\uparrow\uparrow\downarrow\downarrow\uparrow\uparrow$ high-spin ground-state with an average moment of $0.92\mu_B$/atom resulting from the LSD calculations (cf. Table I). On heating the stable ground-state configuration, the lower half of the film undergoes a spin-reorientation transition at about 1000 K to the low-spin $\uparrow\uparrow\downarrow\uparrow\downarrow\downarrow$ configuration [see Fig. 10(a)] and goes reversibly through the maximum in the magnetization before the film becomes paramagnetic. The origin of the magnetization maximum becomes clear when we analyze the layer-resolved magnetic moments $m_i$ and susceptibilities $\chi_i$ [see Figs. 10(a)–10(c)]; on cooling, a ferromagnetic ordering transition occurs first in the surface bilayer at $T_c$ (surface)$\sim$ 1315 K, while the bilayer close to the interface orders only at $T_c$ (interface)$\sim$ 1220 K in an orientation aligned antiferromagnetically relative to the surface layer, resulting in a decrease of the total moment (note that the specific heat and total susceptibility show only a single broad peak). The small difference in the critical temperatures scales rather well with the exchange coupling within the bilayers (see Table II). The magnetic moments in the two central layers do not show critical behavior, but only a slow, almost linear increase.

At higher temperature where the average moments in the central layers are still rather small the low-spin configuration with an antiparallel orientation of the ferromagnetically ordered surface and interface bilayers is apparently entropy stabilized, because it allows for a wider range of spin fluctuations in the interior of the film. As the temperature is lowered, the high-spin configuration becames energetically favored, but the reorientation of the spin in the entire lower half of the film would be possible only by overcoming a substantial barrier. Hence the metastable low-spin configuration is quenched.

### IV. DISCUSSION AND CONCLUSIONS

In the first part of this work we have presented real-space TB-LMTO calculations of the magnetic exchange-pair interactions for fcc Fe films on Cu(100) substrates. Our calculations show that competition between ferro- and antiferromagnetic exchange interactions characteristic for the fcc phase of iron leads to the existence of a variety of metastable low- and high-spin configurations in films with more than 2 ML, confirming earlier results[24,47–49] obtained using different techniques. The calculations of the exchange-pair interactions using a torque-force method leads to rather surprising results: (a) The exchange coupling is strongly enhanced in the boundary layers of the film, both at the free surface and at the interface with the nonmagnetic substrate. The enhancement decreases with increasing thickness of the films. (b) The exchange interactions are drastically reduced in the interior of the films where the moments in neighboring layers are antiferromagnetically aligned. The reduction is strongest for the nearest-neighbor intralayer coupling which almost vanishes in films with 4–6 ML, while the next-nearest-neighbor intralayer and the interlayer coupling remain relatively strong. However, in all cases at least some of the interlayer couplings are frustrated — the ground-state
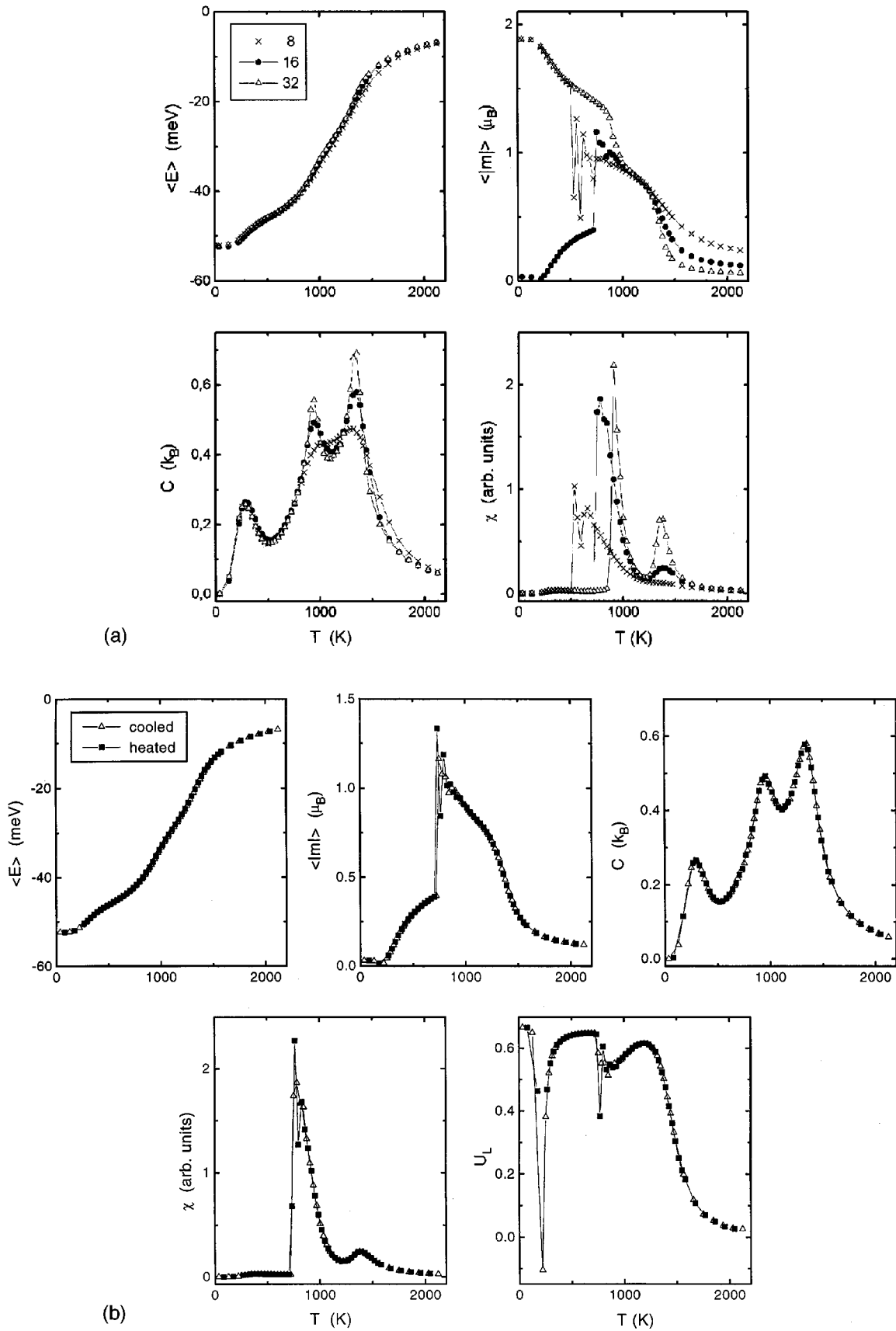
FIG. 7. (a) Temperature dependence of the internal energy $E$, magnetization $M$, specific heat $C$, and susceptibility $\chi$ as recorded in three MC cooling runs for different ensembles representing a 5 ML-Fe/Cu(100) film. (b) Average energy, magnetic moment, specific heat, susceptibility, and cumulant for a $(16 \times 16 \times 5)$ ensemble going reversibly through the spin-reorientation transition. Cf. text.
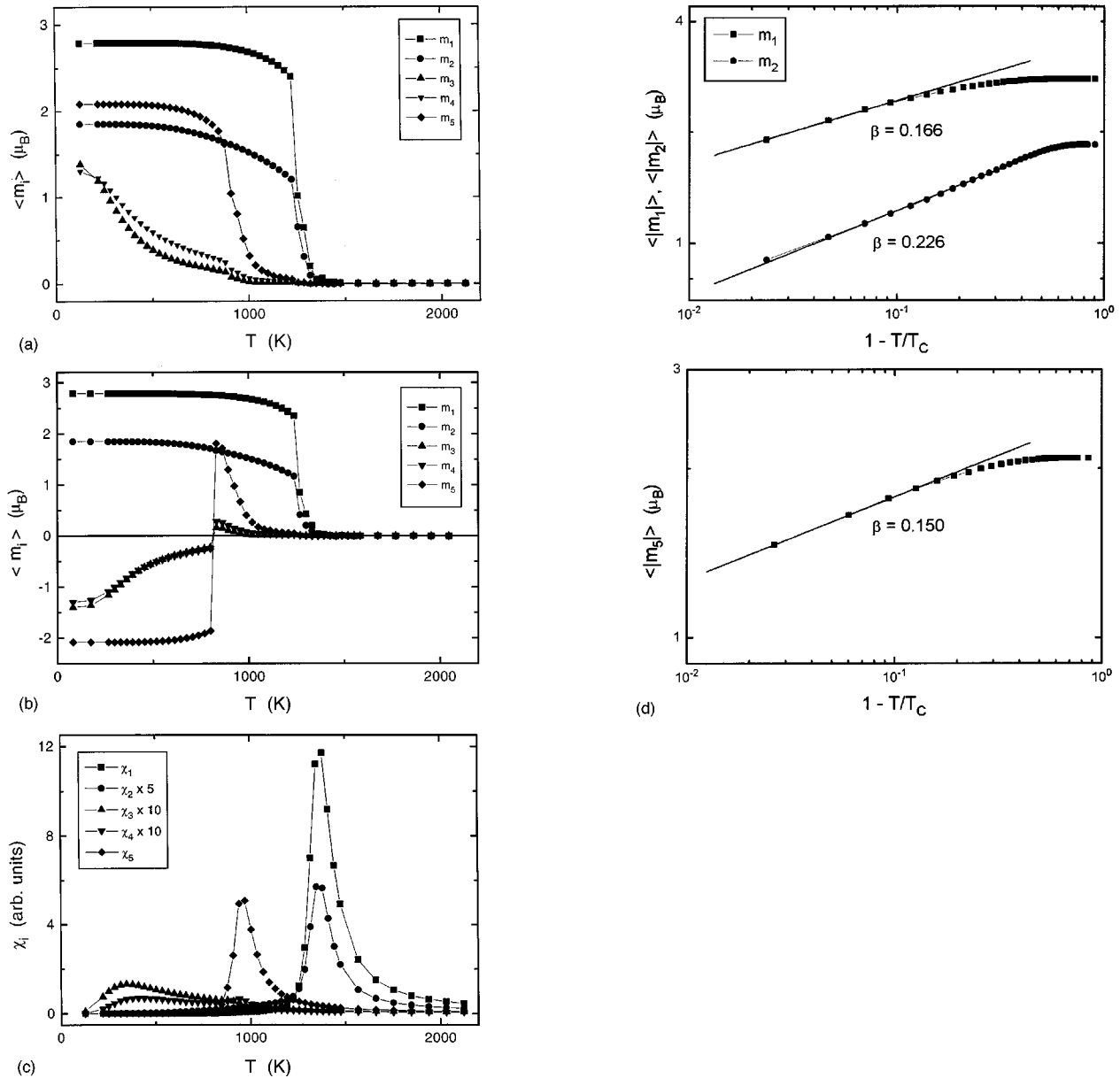
FIG. 8. (a) Temperature dependence of the layer-resolved average moments $\langle m_i \rangle$ for the high-spin PM-FM transition in the 5 ML-Fe/Cu(100) film on cooling. (b) Same for the high-spin–low-spin reorientation transition on heating the $\uparrow\uparrow\downarrow\downarrow\uparrow\uparrow$ configuration. Note that here we plot $\langle m_i \rangle$ and not $\langle |m_i| \rangle$—in this case the transition is more abrupt. (c) Temperature dependence of the layer-resolved susceptibilities $\chi_i$ for the high-spin transition in the 5 ML-Fe/Cu(100) film. Cf. text. (d) Variation of the magnetic moments in the surface and subsurface layer ($m_1, m_2$) and in the interface layer ($m_5$) as a function of the reduced temperature $|1 - T/T_c|$. The straight lines show the linear interpolations used to estimate the critical exponents.

configuration is just the one with the minimal frustrations. (c) Long-range interactions exist at about the same level as in the bulk and close to the surface of a semiinfinite crystal. Hence the exchange interactions in the films are considerably more complex than a simple picture based on a surface-induced enhancement would suggest.

The second part of this study was devoted to a Monte Carlo study of magnetic phase transitions in films with frustrated exchange interactions. However, because of the high computational effort that simulations with long-range Heisenberg-type interactions would require, the simulations were performed for an Ising Hamiltonian with nearest- and next-nearest interactions taken from the TB-LMTO calculations for Fe/Cu(100) films. In principle, the effects of the truncation could be reduced by a renormalization of the strength of the interactions. However, this would essentially reduce the critical temperatures without changing the scenario of the phase transition. We also have to emphasize that the exchange coupling has been determined from infinitesimal rotation of the moments from a ground-state configuration and depend on that configuration. Hence the results of the simulations should be taken as representative for the transitions in a model with frustrated interactions and not be considered as quantitative predictions for Fe/Cu(100).
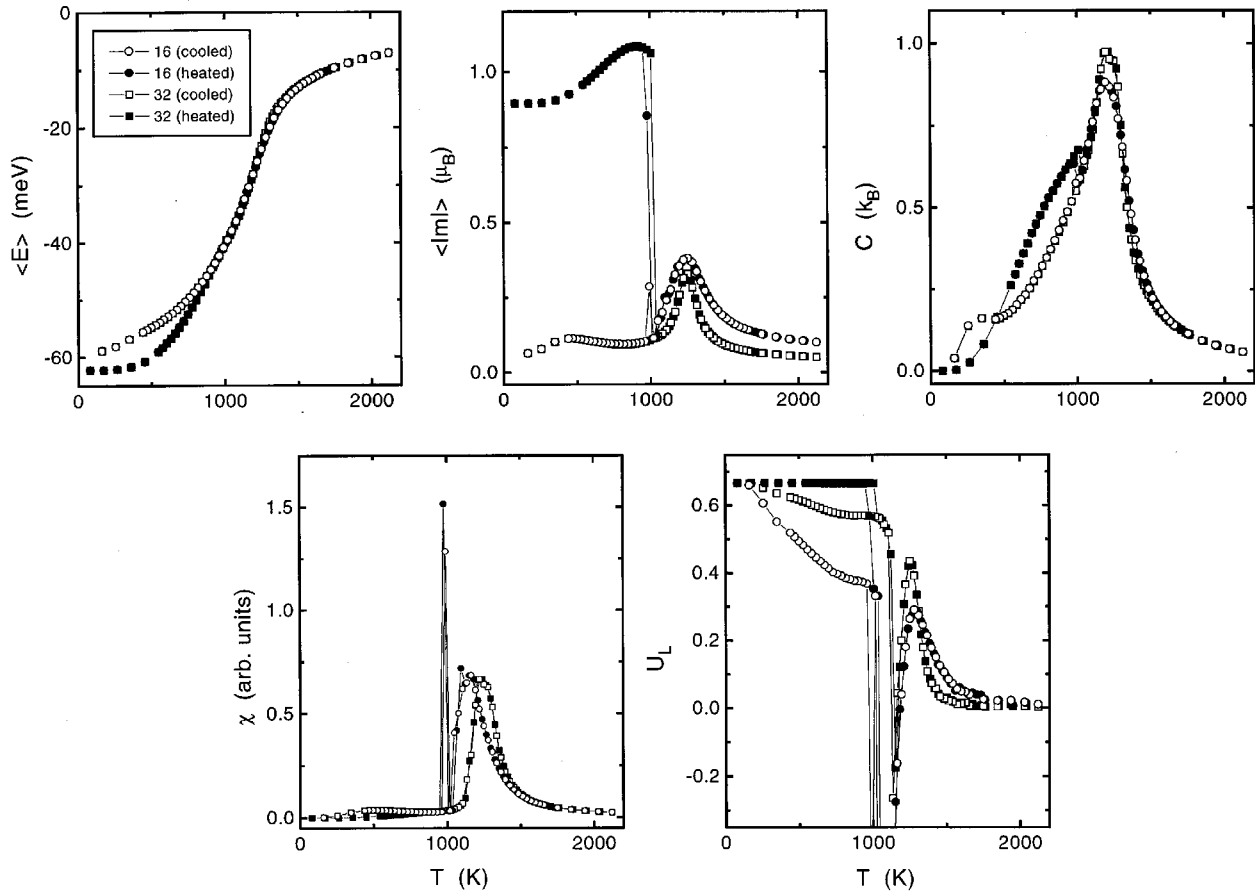
FIG. 9. Variation of the average energy $\langle E \rangle$, the average magnetic moment $\langle |m| \rangle$, specific heat $C$, susceptibility $\chi$, and fourth-order cumulant $U_L$ in a 6 ML-Fe/Cu(100) film. Open symbols: cooling from high temperature, ending in a metastable low-spin $\uparrow\uparrow\downarrow\uparrow\downarrow\downarrow$ configuration. Full symbols: heating from the high-spin $\uparrow\uparrow\downarrow\downarrow\uparrow\uparrow$ ground-state—a spin-reorientation transition in one-half of the film occurs close to $T \sim 1000$ K. Cf. text.

The MC simulations reveal a very complex scenario for the magnetic phase transitions: (a) films with one or two monolayers show a simple paramagnetic-ferromagnetic transition. (b) Films with three monolayers show a paramagnetic-ferromagnetic transition in the surface bilayer, but the antiferromagnetic moment in the interface layer increases only slowly below $T_c$ — this leads to a maximum in the total magnetization just below $T_c$. (c) In a four-monolayer film we find a surface phase transition in the strongly coupled surface bilayer, followed by a somewhat sluggish transition in the interface layer. The moment in the interior of the film increases only very slowly. Altogether this leads to a slow increase of the total moment, as observed experimentally in Fe/Cu(100) films of similar thickness.[15] (d) A similar scenario with two distinct surface and interface phase transitions is also found in 5 ML films. Even after the second phase transition the interior of the film remains essentially nonmagnetic. Once the developing magnetic moments in the interior of the films lead to a coupling of surface bilayer and interface layer, the film can either develop a ferromagnetic high-spin state, or fluctuation effects can lead to a spin-reorientation transition of the lower part of the film to an energetically almost degenerate antiferromagnetic low-spin state. Note that the reorientation transition describes a transition between two different relative orientations of two

two-dimensional ferromagnets that are weakly coupled via the fluctuating moments in the interlayers, and not a genuine phase transition. (e) Surface and interface phase transitions, followed by a fluctuation-induced bifurcation towards high-and low-spin solutions have been found also in the 6 ML films.

Our MC simulations have been performed with an Ising Hamiltonian. Hence they cannot give immediate information on the magnetic anisotropy of the films and its possible variation with temperature. However, the low-spin/high-spin reorientation transitions observed in the 5 and 6 ML films are clearly related to the in-plane/perpendicular reorientation transitions observed in fcc Fe/Cu(100) films with 5–6 ML (Ref. 27): The change of the relative orientations of the ferromagnetic polarization of surface and interface layers influences both the spin-orbit and dipolar contributions to the anisotropy energies (see Ref. 24), but it is not *a priori* clear in which direction (note that both low- and high-moment solutions can appear as low-temperature phases). This point deserves further investigation. Altogether our results show that very large changes in the exchange interactions relative to their values in the bulk can be found in films where a strong ferromagnetic coupling at the surfaces competes with antiferromagnetic interactions in the interior of the films. Such a situation leads to a strong frustration of the pair in-
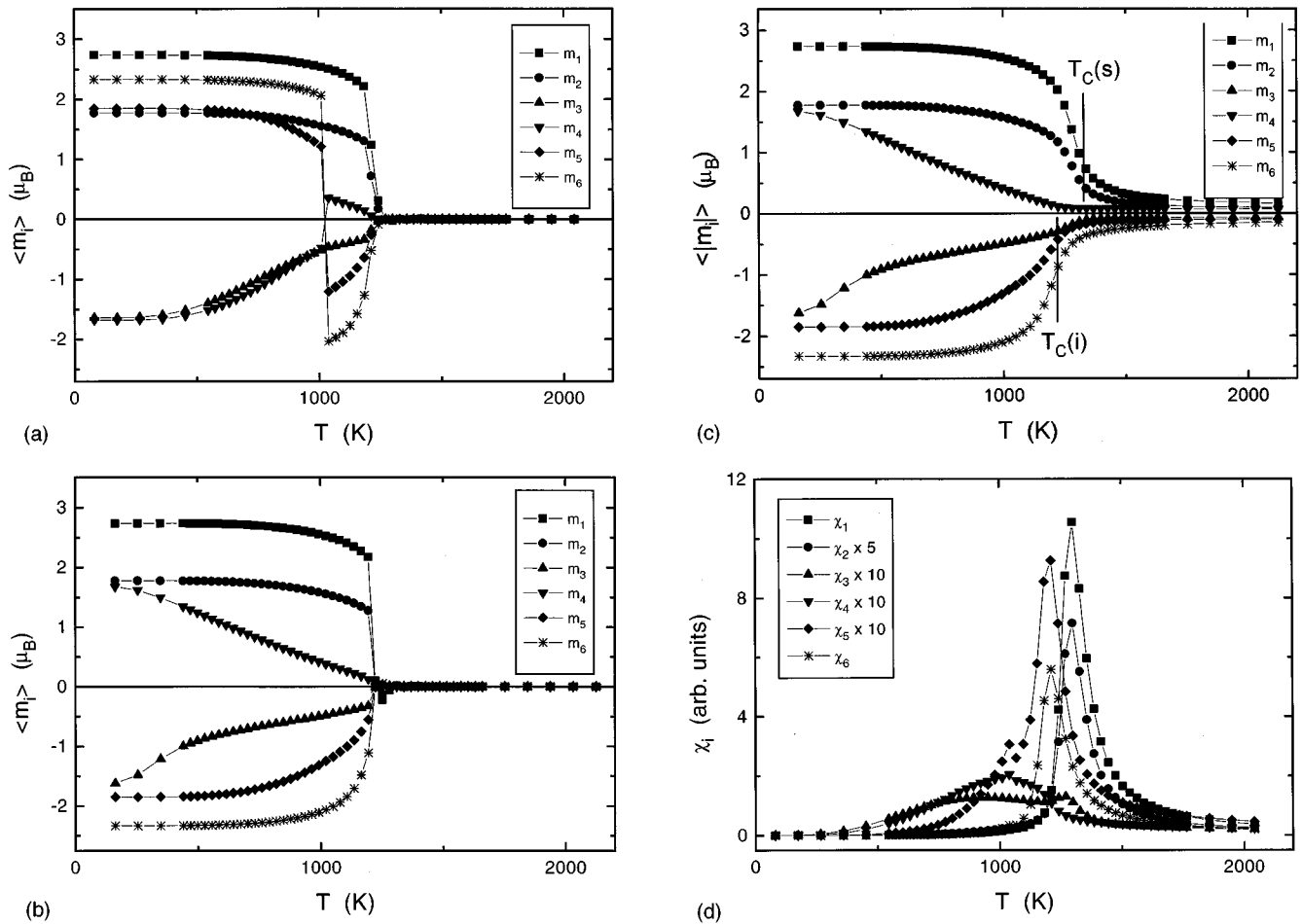
FIG. 10. (a) Variation of the layer-resolved moments $\langle m_i \rangle$ through the spin-reorientation transition on heating. (b,c) Variation of the layer-resolved moments $\langle |m_i| \rangle$ and $\langle m_i \rangle$ during a cooling run. The comparison of these two diagrams shows that the ferromagnetic ordering in the surface bilayer occurs first in small domains with opposite local moments. After the interface bilayer orders ferromagnetically, the fluctuations are effectively suppressed. The critical temperatures for surface and interface phase transitions estimated from the layer-resolved susceptibilities are marked $T_c(s)$ and $T_c(i)$. (d) Layer-resolved susceptibilities $\chi_i$, cf. text.

teractions in the interior of the magnetic film, resulting in the existence of energetically nearly degenerate metastable magnetic configurations and to a decoupling of the magnetic ordering transitions at the surface and at the interface with the substrate from the phase transitions in the inner layers. Our MC simulations show a very rich scenario of surface, interface, and spin-reorientation transitions driven by the frustrated exchange coupling.

### ACKNOWLEDGMENTS

[*]Permanent address: Department of Experimental Physics, Šafárik University, SK 041 54 Košice, Slovak Republic.

[1]K. Binder, in *Phase-transitions and Critical Phenomena*, edited by C. Domb and J. Lebowitz (Academic, London, 1983), Vol. 8, p. 2.

[2]C. Tsallis, in *Magnetic Properties of Low-Dimensional Systems*, edited by L. M. Falicov and J. L. Moran-Lopez (Springer, Heidelberg, 1986).

[3]K. Binder and D. P. Landau, Phys. Rev. Lett. **52**, 318 (1984).

[4]D. P. Landau and K. Binder, Phys. Rev. B **41**, 4633 (1990).

[5]P. Peczak and D. P. Landau, Phys. Rev. B **43**, 1048 (1991).

[6]K. Binder and P. C. Hohenberg, Phys. Rev. B **6**, 3461 (1972); **9**, 2194 (1974).

[7]J. M. Kosterlitz and D. J. Thouless, J. Phys. C **6**, 1181 (1973); J. M. Kosterlitz, *ibid.* **7**, 1046 (1974).

[8]*Ultrathin Magnetic Structures I, II*, edited by B. Heinrich and J. A. C. Bland (Springer, Berlin, 1994); R. Allenspach, J. Magn. Magn. Mater. **129**, 160 (1994), and further references therein.

[9]M. Stampanoni, A. Vaterlaus, M. Aeschlimann, and F. Meier, Phys. Rev. Lett. **59**, 2483 (1957).

[10]M. Przybylski and U. Gradmann, Phys. Rev. Lett. **59**, 1152 (1987).

[11]C. M. Schneider, P. Bressler, P. Schuster, J. Kirschner, J. J. de Miguel, and R. Miranda, Phys. Rev. Lett. **64**, 1059 (1990).

[12]M. E. Fisher, J. Vac. Sci. Technol. **10**, 665 (1973).

[13]D. Weller, S. F. Alvarado, W. Gudat, K. Schröder, and M. Cam-

pagna, Phys. Rev. Lett. **54**, 1555 (1985); D. Weller and S. F. Alvarado, Phys. Rev. B **37**, 9911 (1988).

[14] M. Stampanoni, Appl. Phys. A **49**, 449 (1989).

[15] Th. Detzel, M. Vonbank, M. Donath, N. Memmel, and V. Dose, J. Magn. Magn. Mater. **152**, 287 (1996).

[16] U. Gradmann, Appl. Phys. **3**, 161 (1974).

[17] D. Pescia, M. Stampanoni, G. L. Bona, A. Vaterlaus, R. F. Willis, and F. Meier, Phys. Rev. Lett. **58**, 2126 (1987).

[18] D. Mauri, D. Scholl, H. C. Siegmann, and E. Kay, Phys. Rev. Lett. **62**, 1900 (1990).

[19] C. Rau, Prog. Surf. Sci. **46**, 135 (1994).

[20] P. J. Jensen, H. Dreyssé, and K. H. Bennemann, Europhys. Lett. **18**, 463 (1992).

[21] D. Spišák and J. Hafner, J. Magn. Magn. Mater. (to be published).

[22] D. Spišák and J. Hafner, Phys. Rev. B **55**, 8304 (1997).

[23] S. Blügel, B. Drittler, R. Zeller, and P. Dederichs, Appl. Phys. A **49**, 547 (1989).

[24] R. Lorenz and J. Hafner, J. Magn. Magn. Mater. **157/158**, 514 (1996); Phys. Rev. B **54**, 15 937 (1996).

[25] H. Hasegawa, Surf. Sci. **182**, 591 (1987).

[26] C. Liu, E. R. Moog, and S. D. Bader, Phys. Rev. Lett. **60**, 2422 (1988).

[27] D. P. Pappas, K. P. Kämper, and H. Hopster, Phys. Rev. Lett. **64**, 3179 (1990).

[28] R. Allenspach and A. Bischof, Phys. Rev. Lett. **69**, 3385 (1992).

[29] J. Thomassen, F. May, B. Feldmann, M. Wuttig, and H. Ibach, Phys. Rev. Lett. **69**, 3831 (1992).

[30] Dongqi Li, M. Freitag, J. Pearson, Z. Q. Qiu, and S. D. Bader, Phys. Rev. Lett. **72**, 3112 (1994).

[31] F. Scheurer, R. Allenspach, P. Lhommeux, and E. Courtens, Phys. Rev. B **48**, 9890 (1993).

[32] D. J. Keavney, D. F. Storm, J. W. Freeland, I. L. Grigorov, and J. C. Walker, Phys. Rev. Lett. **74**, 4531 (1995).

[33] R. D. Ellerbrock, A. Fuerst, A. Schatz, W. Keune, and R. A. Brand, Phys. Rev. Lett. **74**, 3053 (1995).

[34] J. Giergiel, J. Shen, J. Woltersdorf, A. Kirilyuk, and J. Kirschner, Phys. Rev. B **52**, 8528 (1995).

[35] W. A. A. Macedo and W. Keune, Phys. Rev. Lett. **61**, 475 (1988).

[36] W. A. A. Macedo, W. Keune, and R. D. Ellerbrock, J. Magn. Magn. Mater. **94**, 552 (1991).

[37] H. Magnan, D. D. Chandesris, B. Villette, O. Heckmann, and J. Lecante, Phys. Rev. Lett. **67**, 859 (1991).

[38] D. D. Chambliss, K. E. Johnson, R. J. Wilson, and S. Chiang, J. Magn. Magn. Mater. **121**, 1 (1993).

[39] S. Müller, P. Bayer, A. Kiene, and K. Heinz, Surf. Sci. **322**, 21 (1995).

[40] S. Müller, P. Bayer, C. Reischl, K. Heinz, B. Feldmann, H. Zillgen, and M. Wuttig, Phys. Rev. Lett. **74**, 765 (1995).

[41] M. Wuttig and J. Thomassen, Surf. Sci. **282**, 237 (1993).

[42] M. Wuttig, B. Feldmann, J. Thomassen, F. May, H. Zillgen, A. Brodde, H. Hannemann, and H. Neddermeyer, Surf. Sci. **291**, 14 (1993).

[43] C. L. Fu and A. J. Freeman, Phys. Rev. B **35**, 925 (1987).

[44] G. N. Fernando and B. R. Cooper, Phys. Rev. B **38**, 3016 (1988).

[45] T. Kraft, P. M. Marcus, and M. Scheffler, Phys. Rev. B **49**, 11 511 (1994).

[46] S. S. Peng and H. J. F. Jansen, J. Appl. Phys. **69**, 6132 (1991).

[47] R. Lorenz and J. Hafner, Thin Solid Films **281**, 492 (1996).

[48] B. Ujfalussy, L. Szunyogh, and P. Weinberger, Phys. Rev. B **54**, 9883 (1996).

[49] L. Szunyogh, B. Ujfalussy, and P. Weinberger, Phys. Rev. B **55**, 14392 (1997).

[50] R. Lorenz and J. Hafner, Phys. Rev. Lett. (to be published).

[51] U. von Barth and L. Hedin, J. Phys. C **5**, 1629 (1972).

[52] O. K. Andersen and O. Jepsen, Phys. Rev. Lett. **53**, 2571 (1984).

[53] O. K. Andersen, O. Jepsen, and M. Šob, in *Electronic Band Structure and its Applications*, edited by M. Yussoff (Springer, Berlin, 1987).

[54] S. K. Bose, S. S. Jaswal, O. K. Andersen, and J. Hafner, Phys. Rev. B **37**, 9955 (1988).

[55] R. Haydock, V. Heine, and M.J. Kelly, in *Solid State Physics: Advances in Research and Applications,* edited by H. Ehrenreich and D. Turnbull (Academic, New York, 1980), Vol.35.

[56] N. Beer and D. G. Pettifor, in *The Electronic Structure of Complex Systems*, edited by P. Phariseau and W. M. Temmerman (Plenum, New York, 1984).

[57] L. M. Small and V. Heine, J. Phys. F **14**, 3041 (1984).

[58] O. N. Mryasov, A. J. Freeman, and A. I. Liechtenstein, J. Appl. Phys. **79**, 4805 (1996).

[59] R. Lorenz and J. Hafner, J. Magn. Magn. Mater. **139**, 209 (1995).

[60] O. N. Mryasov, V. A. Gubanov, and A. I. Liechtenstein, Phys. Rev. B **45**, 12 330 (1992).

[61] M. Uhl, L. M. Sandratskii, and J. Kübler, J. Magn. Magn. Mater. **45**, 314 (1992).

[62] D. Spišák and J. Hafner (unpublished).

[63] K. Binder and D. Stauffer, in *Applications of the Monte Carlo Method in Statistical Physics*, edited by K. Binder (Springer, Berlin, 1987), p. 1.

[64] K. Binder, Z. Phys. B **43**, 119 (1981).